Mechanics & Industry **25**, 18 (2024)

https://doi.org/10.1051/meca/2024013

Mechanics & Industry

Available online at:
www.mechanics-industry.org

Original Article

Open Access

A method to manufacture spiral bevel gears by equivalent completing

Longlong Geng[1,2*], Shaowu Nie[1], and Chuang Jiang[1]

[1] School of Mechatronics Engineering, Henan University of Science and Technology, 48, Xiyuan Road, Luoyang 471003, China
[2] Zhejiang Tongli Transmission Technology Co., Ltd, Wenzhou, Zhejiang 325000, China

Received: 7 December 2023 / Accepted: 29 April 2024

Abstract. As a transmission part for industrial application the manufacture of spiral bevel gear is particularly important. The present machining methods for manufacturing spiral bevel gears, including the so called five-cut method and completing method, have drawbacks such as low processing efficiency, requiring complex calculations and high requirements on the machine-tool performance, respectively. To solve the above problems, an equivalent completing method is proposed to process spiral bevel gear in this paper. Firstly the machine setting parameters by completing were translated from the Cradle-type hypoid generator to Cartesian-type hypoid generator and the workpiece is swing during process. CNC motion axes expression of Cartesian-type hypoid generator were expressed as sixth-order polynomial, the influences of coefficient on the tooth surface topology were researched. Then the method to machine spiral bevel gear was put forward by reducing the swing axis of workpiece, obviously a deviation of tooth surface was caused between theoretical and axis-reduced. As a response, a flank correction model was established and the other polynomial coefficients were adjusted to eliminate the deviation. Finally simulation and cutting experiment were carried out by a numerical example. The experimental results show that the proposed method is effective and feasible. The method proposed in this paper overcome and enrich the disadvantages of existing manufacture methods of spiral bevel gear.

Keywords: Spiral bevel gear / face-milling / equivalent completing / simulation / cutting experiment

1 Introduction

Spiral bevel gears are widely used in vehicle, aircraft and industrial gearbox to transmit rotation between intersecting axes for its advantages of smoothly driving, high transmission efficiency, excellent load capacity, etc. So manufacture technology of spiral bevel gear is always a focus topic for experts and scholars to research. Therefore, many researches are carried out. Currently, the main way to machine spiral bevel gears is face-milling which is divided into five-cut method and completing method according to the process of pinion. Traditionally, a pair of spiral bevel gears are manufactured by rough machining of wheel, rough machining of pinion, finish machining of wheel, finish machining of pinion concave side and convex side respectively, so it is named five-cut method. Generalized theory of spiral bevel gears manufactured by five-cut method have been comprehensively presented by several gear scientists [1,2]. Shtipelman [3] introduced generalized theory of five-cut method and derived general formulas for calculating the basic machine-tool settings of spiral bevel gears designed and manufactured by Gleason Works. Litvin [4,5] developed the generalized theory and calculation for five-cut method independently that is different from Gleason's technology. Muhammad [6] developed a mathematical model to calculate the cutter system location, and then established the machine kinematics chain of a typical machine tool of variable specification to compute the coordinates of the machine axes in face milling. Completing method was firstly proposed (also known as duplex helical method) to machine spiral bevel gear by Gleason [7]. For completing method, the concave side and convex side of pinion are simultaneously machined. At the same time the rough and finish machine of wheel and pinion are unified separately. However the cutting principle and calculation of machine setting were not fully revealed. Litvin et al. [8] suggested the helixform and formate methods for hypoid gears. Zhang et al. [9] revealed the cutting principle and calculated the basic machine-tool settings for spiral bevel and hypoid gears by duplex helical method. Geng et al. [10] presented a method to predesign contact path by duplex helical method which guaranteed contact performance. The above literates are the latest research to machine spiral bevel gears by completing method that achieve active design of mesh performance.

* e-mail: gll0379@haust.edu.cn

For five-cut method, the usage of machine tool and space are large, and workpiece has to install in multiple which inevitably increases the installation error, whereas design and modification of tooth surface are flexible for concave side and convex side are independent. For completing method, not to say the calculation process is complex, there are also harsh requirements for machine tool and cut tools, although it can realize efficient processing. Other processing methods were also explored. Deng et al. [11] presented a machining method for face milling using a disk cutter with a concave end by 5-axis computerized numerical control (CNC) machine tool, this is also an effective method while its efficiency is not suitable for mass production. So, it is imminent to put forward a new method to machine spiral bevel gear which is not too harsh requirements for machine tools or existing machine tools can meet requirements.

Soon afterwards, Geng et al. [12] proposed duplex spread blade method to manufacture spiral bevel gear by based on 4-axis CNC milling machine, and tooth flank was modified to optimize mesh performance. Then a helical correction motion was introduced to manufacture spiral bevel gear to optimize contact patterns [13]. The above researches prove that four-axis linkage CNC machine tool can achieve the double-sided machining of spiral bevel gears. However, the above processing has certain limitations such as strict requirements for cutter size and mesh performance is not well guaranteed. Deng et al. [14] proposed the method to process two sides of pinion tooth surface with the same cutter head which the tooth length curvature was corrected according to the characteristic that NC machine tool can adjust cutter location in real time. With the development of NC technology, higher order motion was applied to machine spiral bevel gear. Stadtfeld [15] proposed universal motion concept (UMC) and made it possible to realize the desired contact pattern and motion graph characteristics. Fong [16] clearly showed the method applying modified radial motion to achieve the predetermined fourth-order motion curve and contact pattern. Fan [17] and Ship [18] proposed a method of tooth flank error correction utilizing the high-order universal motions for spiral bevel and hypoid gears by face-milling process to meet the increasing demand for low noise and high strength leads to high quality requirement. Ship [12] proposed a flank-correction methodology derived directly from the six-axis Cartesian-type CNC hypoid generator in which the motion axis were presented as sixth-order Taylor polynomials in terms of the cradle rotation angle. The higher order motion of NC axis can develop potential of machine tools. As the machine-tool setting parameters transferred to Cartesian-type CNC (as shown in Fig. 1), the axle of machine root angle is swing as the workpiece manufactured.

Unfortunately the motion of machine root angle reduces machine rigidity and the precision of movement is difficult to ensure [19]. Yang et al. [20] presented an active design and manufacture of spiral bevel gear by completing method with fixed workpiece axis based on a free-form machine tool. Nie et al.[21] proposed a kind of pinion flank modification method without tilt processing based on equivalent tooth flank mismatch to achieve the equivalent pinion processing with tilt on no tilt machine by five-cut method. Ship [22] proposed a face-milling system

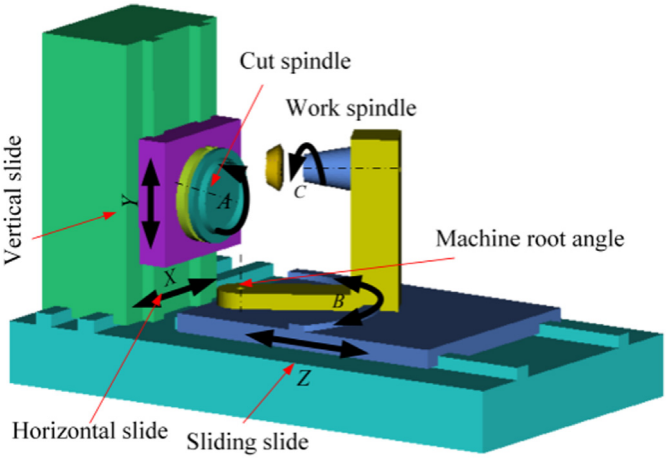

Fig. 1. Schematic of Cartesian-type milling machine tool.

with flank correction for bevel gears on a five-axis CNC machine in which wheel was corrected for concave side and convex side, respectively. It is possible to machine both tooth surfaces of pinion with one clamp by set the tilt angle as zero and modify the other machine-tool parameters when tilt angle is small by completing method.

Based on the previous research [10,14] and inspiration of the above literature, an equivalent completing method is proposed by dedicated spiral bevel gear milling machine in this paper. Concave side and convex side of pinion are machined separately in one clamp like completing method by optimize tool path. Then the problem that it is difficult to modify and correct the tooth surface by completing method is solved. So the method is named equivalent completing, which also overcomes the strict requirements for machine tools by completing method and the inconsistency of the workpiece caused by multiple installations by five-cut method. And the main scheme is shown in Figure 2.

As Figure 2 displays, firstly machine setting parameters are converted from Cradle-type to Cartesian-type machine tool and the motion axes are expressed in the form of sixth order polynomial, the tooth surface according to sixth order polynomial of (X,Y,Z,A,B) is defined as theory tooth surface. Then let machine root angle as a constant, a tooth surface according to the sixth order polynomial of (X,Y,Z,A) and machine root angle is defined as real tooth surface. Tooth surface deviation is calculated between theory and real tooth surface. To reduce the deviation, influence of polynomial coefficients on tooth surface is researched and a tooth surface correction method is proposed by adjust polynomial coefficient of (X,Y,Z). After correction the expressions of sixth order polynomials for concave side and convex side are different, the machine process are simulated and the NC program is specially designed to realize concave side and convex side machining in one clamp.

2 Equivalent conversion

The mathematical model of Cradle-type by completing method is showed in Figure 3. $S_m(X_m, Y_m, Z_m)$is the machine tool coordinate system. The cutter position is

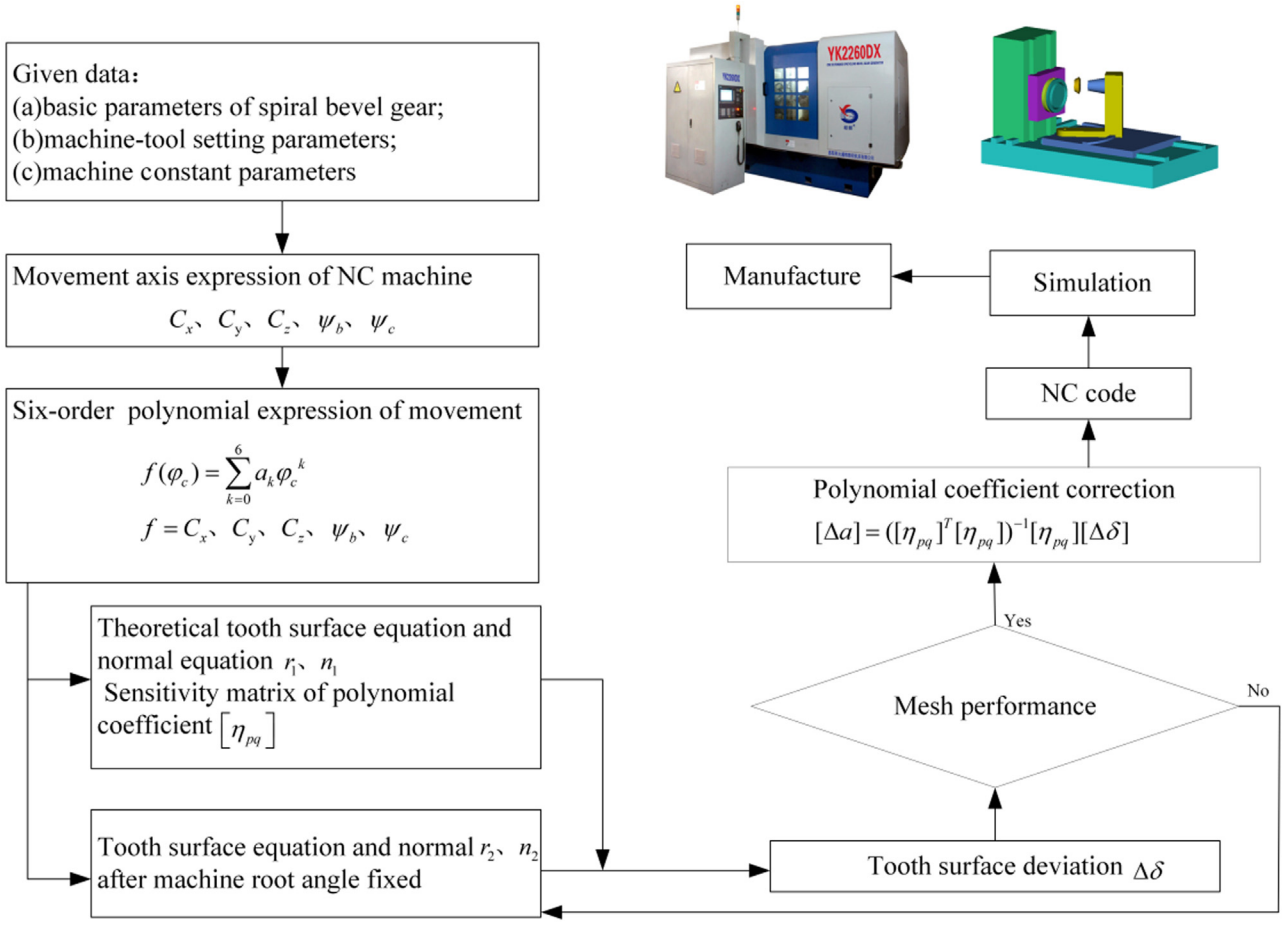

Fig. 2. Flow chart to machine spiral bevel gear by equivalent completing method.

determined by tilt angle i, swivel angle i, radial setting S_r, initial cradle angle setting q. The position of workpiece is determined by vertical offset E_m, sliding base X_B helical motion H machine root angle γ, machine center to back X_g. $S_c(X_c, Y_c, Z_c)$ is coordinate system of cradle which rotates with the cradle during process, and φ_c is the angle of X_c relative to X_m $S_w,(X_w, Y_w, Z_w)$is coordinate system of workpiece, and ϕ is the angle of workpiece during process. R_a is rolling ratio which determines the relative motion relationship between cradle and workpiece and satisfies $\phi=R_a\varphi_c$. A great difference from the five-cut method is that a spread-blade cutter is used for pinion finish machine as completing method. And the cutter model is showed in Figure 4.

As Figure 4 shows, the spread-blade cutter made up of the inner cut and outer cut. The equation of cut in the cutter coordinate system can be represented as

$$r_t = [(r_{1i} + u\sin\alpha_{1i})\cos\theta - (r_{1i} + u\sin\alpha_{1i})\sin\theta\, u\cos a\, 1] \quad (1)$$

where i represents the inner cut or outer cut, for i=1 represents outer cut, for i=2 represents inner cut. μ is the position of the point in the blade, θ is the rotation angle of cutter.

Then tooth surface can be obtained by coordinate transformation in Cradle-type machine

$$\begin{aligned}\mathbf{r}_w(u,\theta,\varphi_c,\psi_m) &= \mathbf{M}_{we}\mathbf{M}_{ed}\mathbf{M}_{dc}\mathbf{M}_{cG}\mathbf{M}_{Gb}\mathbf{M}_{ba}\mathbf{M}_{at}\mathbf{r}_t \\ &= \mathbf{M}_{wt}\mathbf{r}_t \end{aligned} \quad (2)$$

where ψ_m represents the machine setting parameters. M_{wt} is matrix for coordinate transform from S_t to S_w.

$$M_{we} = \begin{bmatrix} 1 & 0 & 0 & 0 \\ 0 & \cos\phi & -\sin\phi & 0 \\ 0 & \sin\phi & \cos\phi & 0 \\ 0 & 0 & 0 & 1 \end{bmatrix}$$

$$M_{ed} = \begin{bmatrix} \cos\gamma_m & 0 & \sin\gamma_m & -X_g \\ 0 & 1 & 0 & 0 \\ -\sin\gamma_m & 0 & \cos\gamma_m & 0 \\ 0 & 0 & 0 & 1 \end{bmatrix}$$

$$M_{dc} = \begin{bmatrix} 1 & 0 & 0 & 0 \\ 0 & 1 & 0 & E_m \\ 0 & 0 & 1 & -X_B \\ 0 & 0 & 0 & 1 \end{bmatrix}$$

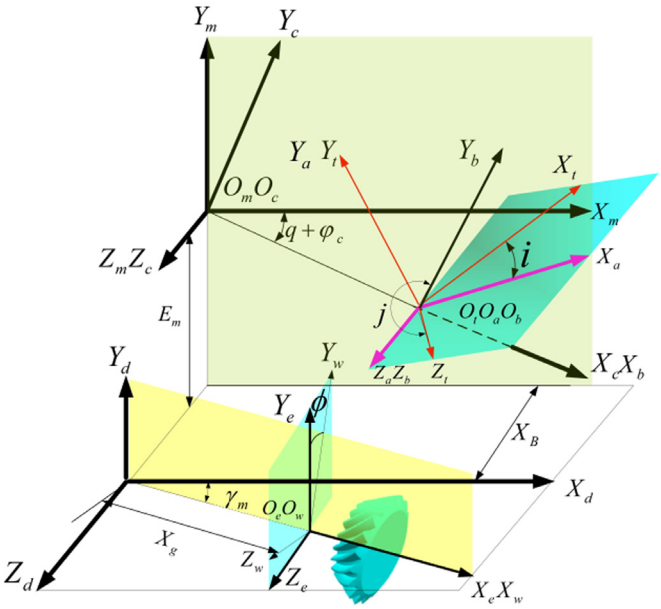

Fig. 3. Mathematical model of Cradle-type machine.

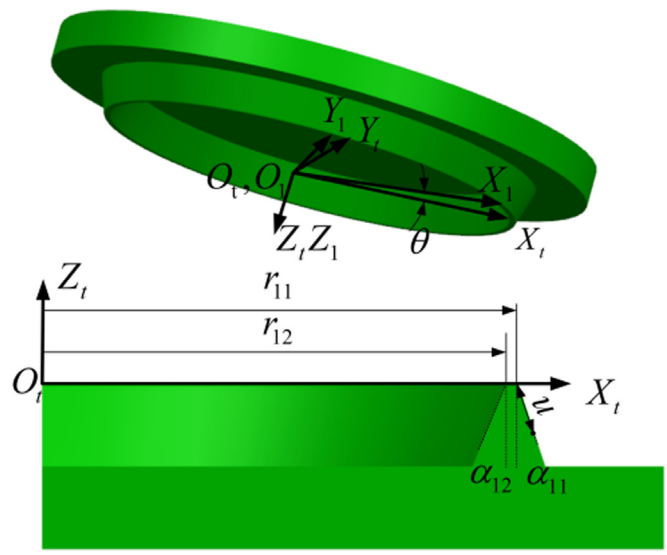

Fig. 4. Model of spread-blade cutter.

$$M_{cG} = \begin{bmatrix} \cos\varphi_c & -\sin\varphi_c & 0 & 0 \\ \sin\varphi_c & \cos\varphi_c & 0 & 0 \\ 0 & 0 & 1 & 0 \\ 0 & 0 & 0 & 1 \end{bmatrix}$$

$$M_{Gb} = \begin{bmatrix} \cos q & -\sin q & 0 & 0 \\ \sin q & \cos q & 0 & 0 \\ 0 & 0 & 1 & 0 \\ 0 & 0 & 0 & 1 \end{bmatrix}$$

$$M_{ba} = \begin{bmatrix} -\sin j & -\cos j & 0 & S_r \\ \cos j & -\sin j & 0 & 0 \\ 0 & 0 & 1 & 0 \\ 0 & 0 & 0 & 1 \end{bmatrix}$$

$$M_{at} = \begin{bmatrix} \cos i & 0 & \sin i & 0 \\ 0 & 1 & 0 & 0 \\ -\sin i & 0 & \cos i & 0 \\ 0 & 0 & 0 & 1 \end{bmatrix}.$$

Mathematical model of Cartesian-type machine was established as Figure 5, $S_w(X_w, Y_w, Z_w)$ the coordinate system of workpiece. C_x, C_y determine the position of cut, C_z ensure the tooth surface and the tooth depth. ψ_c is the rotation of workpiece, ψ_b is the angle of workpiece installed, C_d is the distance between the origin of the machine and pitch cone of workpiece, $\Delta\psi_c$ is an additional angle of workpiece during manufacture.

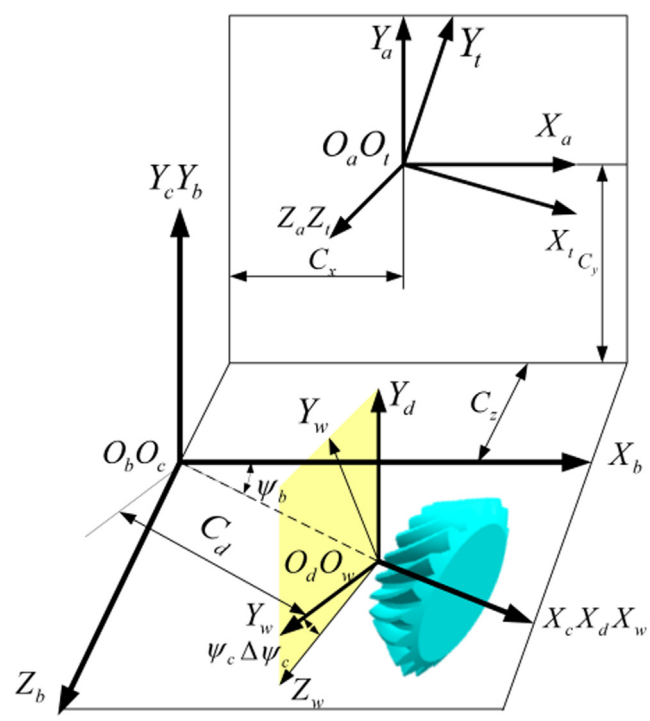

Fig. 5. Mathematical model of Cartesian-type machine.

Then tooth surface can be obtained by coordinate transformation in Cartesian-type machine as

$$\begin{aligned} \boldsymbol{r}_w &= \boldsymbol{M}_{wd}\mathbf{M}_{dc}\boldsymbol{M}_{cb}\boldsymbol{M}_{ba}\boldsymbol{r}_t \\ &= \boldsymbol{M}_{wt}(C_x, C_y, C_z, \psi_b, \psi_c{+}\Delta\psi_c)\boldsymbol{r}_t, \end{aligned} \tag{3}$$

where

$$\boldsymbol{M}_{ba} = \begin{bmatrix} 1 & 0 & 0 & C_x \\ 0 & 1 & 0 & C_y \\ 0 & 0 & 1 & -C_z \\ 0 & 0 & 0 & 1 \end{bmatrix}$$

$$\boldsymbol{M}_{cb} = \begin{bmatrix} \cos\psi_b & 0 & \sin\psi_b & 0 \\ 0 & 1 & 0 & 0 \\ -\sin\psi_b & 0 & \cos\psi_b & 0 \\ 0 & 0 & 0 & 1 \end{bmatrix}$$

$$\boldsymbol{M}_{dc} = \begin{bmatrix} 1 & 0 & 0 & -C_d \\ 0 & 1 & 0 & 0 \\ 0 & 0 & 1 & 0 \\ 0 & 0 & 0 & 1 \end{bmatrix}$$

$$\boldsymbol{M}_{wd} = \begin{bmatrix} 1 & 0 & 0 & 0 \\ 0 & \cos(\psi_c+\psi_c) & -\sin(\psi_c+\psi_c) & 0 \\ 0 & \sin(\psi_c+\psi_c) & \cos(\psi_c+\psi_c) & 0 \\ 0 & 0 & 0 & 1 \end{bmatrix}$$

where M_{wt} is matrix for coordinate transform from S_t to S_w.

No matter the Cradle-type or Cartesian-type is used to manufacture the pinion, the relative motion relationship between cutter and workpiece is the same. So based on the above principle, the machine-tool setting parameters of Cradle-type was transformed to the movement expression of Cartesian-type, further the movement expression were expanded into a polynomial of sixth order.

According to (2) and (3), matrix for coordinate transform M_{wt} is equal, and then the movement expression can be calculated and expanded into a polynomial of the sixth order in φ_c=0.

$$\begin{aligned} f(\varphi_c) &= \sum_{k-0}^{6} a_k \varphi_c^k \\ f &= C_x, C_y, C_z, \psi_b, \psi_c \end{aligned} . \tag{4}$$

The tooth surface equation can be obtained by substitute (4) into (3). Then the normal vector $\boldsymbol{n_w}$ in the workpiece coordinate system can be expressed as

$$\boldsymbol{n}_w(u,\theta,\phi_c) = \frac{\dfrac{\partial \boldsymbol{r}_w(u,\theta,\phi_c)}{\partial u} \times \dfrac{\partial \boldsymbol{r}_w(u,\theta,\phi_c)}{\partial \theta}}{\dfrac{\partial \boldsymbol{r}_w(u,\theta,\phi_c)}{\partial u} \times \dfrac{\partial \boldsymbol{r}_w(u,\theta,\phi_c)}{\partial \theta}} . \tag{5}$$

The meshing equation in the workpiece coordinate system can be expressed as

$$f(u,\beta,\phi_c) = \boldsymbol{n}_w . v = \boldsymbol{n}_w . \frac{\partial \boldsymbol{r}_w(u,\theta,\phi_c)}{\partial \phi_c} . \tag{6}$$

Table 1. Basic parameters.

Parameter	Pinion	Gear
Shaft angle Σ (°)	90	
Module (mm)	7.16	
Pressure angle β (°)	20	
Spiral bevel angle α (°)	35	
Width $_b$ (mm)	50	
Tooth number $_z$	18	35
Pitch cone angle δ (°)	27.21611	62.78333
Face cone angle δ_a (°)	32.65	64.6333
Root cone angle δ_f (°)	25.367	57.35
Addendum h_{ae} (mm)	8.78	3.55
Dedendum $_{fe}$ (mm)	5.03	10.26
Constant of machine (mm)	80	
Fixture length (mm)	167.8	
Mounting distance (mm)	130	90

The tooth surface can be numerically represented by a series of surface point. The points are defined in the axial plane *XL-RL* of pinion that *XL* is coincide with axis of pinion.

$$\begin{aligned} XL &= r_w(1) \\ RL &= \sqrt{r_w^2(2) + r_w^2(3)} \end{aligned} . \tag{7}$$

According to (4)–(7), the points of tooth surface can be obtained. An example was applied to calculate the motion axes polynomial expression, only the pinion was presented in this paper. The basis parameters of spiral bevel gear are listed in Table 1, the machine-tool setting parameters by completing method are listed in Table 2.

The motion axes of sixth-order polynomial expression of 5-axis NC machine were calculated by (2)–(4) and showed in Table 3.

3 Mathematical of equivalent completing

The mathematical model of Cartesian-type CNC was made up of three linear axes (X, Y, Z) and three revolving axes (A, B, C) as showed in Figure 1. As literature [12] analyzed, the axis of machine root angle $\psi_b(\varphi_c)$ was swing as workpiece manufactured after the machine setting parameters were transferred. It is not essential for interpolation of cut spindle A by face-milling and an appropriate speed meets the requirements. Then in this paper based on the purpose of eliminating the unnecessary function and reducing the cost of machine, a simplified mathematical model was established. Three linear axes (X, Y, Z) and revolving axis (C) that the workpiece was installed are with multiple axis control simultaneously. During process, the cut spindle (A) can be derived by an ordinary motor which drive the cut at a proper speed. And the machine root angle (B) is manual adjustment. Then a matter of course, a tooth surface deviation was generated. In order to reduce tooth

Table 2. Machine-tool setting parameters.

Parameter		Pinion	Gear
Tilt angle i (°)		2.90	0
Swivel angle j (°)		173.42	205.73
Radial setting s_r (mm)		106.1841	107.3358
Initial cradle angle setting q (°)		59.53	60.73
Vertical offset E_m (mm)		–0.5295	0
Sliding base X_B (mm)		–0.4075	0.6834
helical motion H (mm/rad)		–1.6905	0
Machine root angle γ (°)		27.80	58.34
Machine center to back X_g (mm)		–0.5311	0
Roll ratio R_a		2.168931	1.121120
Point radius r (mm)	Outer cut	114.865	115.95
	Inner cut	111.865	112.65
Profile angle a (°)	Outer cut	18	18
	Inner cut	22	22

Table 3. Motion axes polynomial expression of pinion.

Items	Polynomial expression
Cx	$53.39858 + 89.87541.\varphi_c - 24.87041\varphi_c^2 - 14.19634\varphi_c^3 - 1.66113\varphi_c^4 + 0.56962\varphi_c^5 + 0.02441\varphi_c^6$
C_y	$-92.58567 + 51.68464.\varphi_c + 44.10242.\varphi_c^2 - 7.684497.\varphi_c^3 - 3.301359.\varphi_c^4 + 0.2497748.\varphi_c^5 + 0.0678956.\varphi_c^6$
C_z	$-0.0279196 + 0.810046.\varphi_c - 0.0054436.\varphi_c^2 + 0.0056869.\varphi_c^3 + 0.000453.\varphi_c^4 - 0.000284.\varphi_c^5 - 0.000015.\varphi_c^6$
C_b	$0.438818 + 0.02002.\varphi_c + 0.02270.\varphi_c^2 - 0.00312.\varphi_c^3 - 0.00179.\varphi_c^4 + 0.00012.\varphi_c^5 + 0.00005.\varphi_c^6$
C_c	$-0.0226356 - 2.132488.\varphi_c + 0.01056.\varphi_c^2 + 0.00807.\varphi_c^3 - 0.00066.\varphi_c^4 - 0.000316.\varphi_c^5 + 0.0000028.\varphi_c^6$

surface deviation, the coefficients of six-order movement expression of X, Y, Z, A were adjusted. The adjustment process of coefficients is as follows.

3.1 Deviation calculation

The tooth surface obtained by Equation (4) was defined as theoretical tooth surface. Let $\psi_b(\varphi_c)$ was a constant, and then a tooth surface can be calculated named as real tooth surface. Obviously, a deviation was occur between theoretical and real tooth surface, the deviations can be calculated as shown in Figure 6.

As Figure 6 shows in S_w, Σ_1 (blue) is theoretical tooth surface, Σ_2 (red) is real tooth surface, Σ_3(red) is real tooth surface after rotation. Firstly, real tooth surface was rotated let the middle of tooth surface M coincide with the theoretical tooth surface M. The angle can be calculated as

$$\begin{pmatrix} x_m \\ y_m \\ z_m \end{pmatrix} = \begin{pmatrix} 1 & 0 & 0 \\ 0 & \cos\theta & -\sin\theta \\ 0 & \sin\theta & \cos\theta \end{pmatrix} \begin{pmatrix} x'_m \\ y'_m \\ z'_m \end{pmatrix}. \quad (8)$$

Grid points on tooth surface can be expressed as $P'(x_w,y_w,z_w)$, after rotation grid points on the tooth surface Σ_3 can be expressed as $P'(x_w,'y_w,'z_w')$. Corresponding

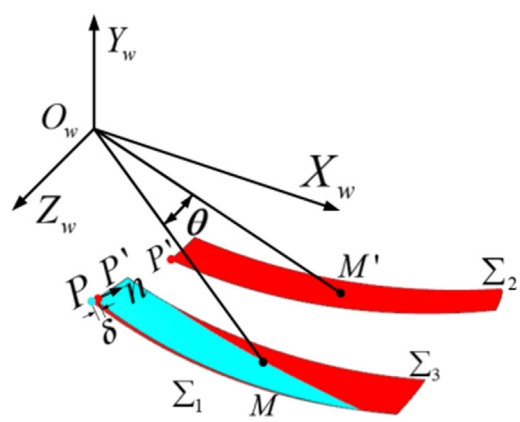

Fig. 6. Tooth surface deviation.

points on the tooth surface Σ_1 were expressed as $P(x_w(u,\theta,\phi_c)$, $y_w(u,\theta,\phi_c)$, $z_w(u,\theta,\ \phi_c)$, and the unit normal vectors were expressed as $(n_w(u,\theta,\phi_c),n_w(u,\theta,\phi_c),\ n_w(u,\theta,\ \phi_c))$.

Then the deviations of grid points can be obtained by

$$\begin{cases} x_w(u,\theta,\phi_c) + \Delta\delta\cdot n_w(u,\theta,\phi_c) = x_w{}' \\ y_w(u,\theta,\phi_c) + \Delta\delta\cdot n_w(u,\theta,\phi_c) = y_w{}' \\ z_w(u,\theta,\phi_c) + \Delta\delta\cdot n_w(u,\theta,\phi_c) = z_w{}' \end{cases}. \quad (9)$$

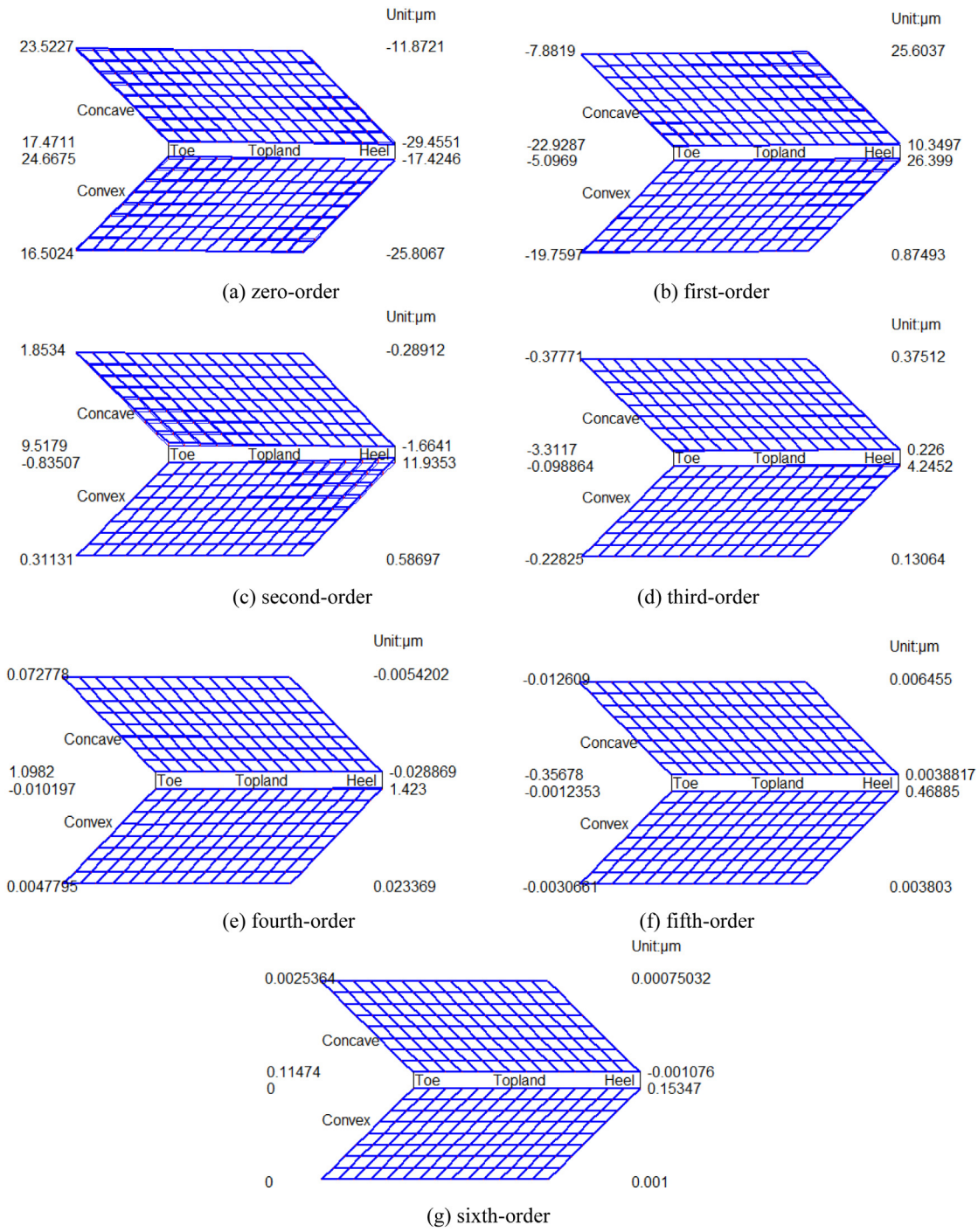

Fig. 7. Influence of polynomial coefficient on tooth topology of Y axis.

3.2 Influence on tooth surface topology analysis

In order to reduce tooth surface deviation through adjust polynomial coefficients, it is necessary to clarify the influence of coefficients on tooth surface topology firstly. Tooth surface deviations are calculated corresponding to change of coefficients by single variable method (in this paper, the change was selected as 0.1mm for the linear axis and 0.1° for revolving axis). And only the results of Y axis were listed in Figure 7.

As Figure 7 shows, (a)–(g) is the tooth surface deviations corresponding to the change of polynomial coefficient from zero-order to sixth-order. The corresponding maximum tooth surface deviations are respectively 29.4511 μm, 26.399 μm, 11.9353 μm, 4.2452 μm, 1.432 μm, 0.46885 μm, 0.15347 μm. It is not difficult to find that along with the increase of polynomial coefficient's order, the deviations become small. The change of the coefficient mainly causes the error of tooth surface helix angle. At the same time, the influence trend on the pressure angle from

Table 4. Weight analysis of Y axis polynomial coefficients on tooth surface topology.

Order	$a_1\times10^{-3}$		$a_2\times10^{-3}$		$a_3\times10^{-3}$		$a_4\times10^{-3}$		$a_5\times10^{-3}$	
	Convex side	Concave side	Convex side	Concave side	Convex side	Concave side	Convex side	Concave side	Convex side	Concave side
Zero	2.838	−0.495	5.583	−14.680	−0.196	−0.008	0.013	−0.029	0.128	−0.120
First	−2.683	0.605	−3.714	−6.232	−0.079	−0.111	0.057	−0.011	0.104	−0.041
Second	−0.611	0.209	3.006	−0.849	−0.045	−0.065	0.011	−0.013	0.016	−0.052
Third	0.129	0.045	−0.704	−0.219	0.007	−0.022	−0.001	−0.005	−0.000	−0.019
Fourth	−0.072	0.016	0.248	−0.042	−0.003	−0.008	0.001	−0.002	0.001	−0.007
Fifth	0.025	0.006	−0.076	−0.008	0.001	−0.003	−0.000	−0.001	−0.000	−0.002
Sixth	−0.009	0.002	0.025	−0.001	−0.000	−0.001	0.000	−0.000	0.000	−0.001

the middle point of the tooth width to heel and toe is opposite, forming bias deviation in different directions. Taking Figure 7a as an example, the concave surface forms a bias angle from toe of topland to heel of root. The convex surface is exactly opposite to the concave surface. For the change of fifth-order, the biggest deviation is less than 1 μm, which is approximately believed that there is no effect on the tooth surface.

From Figure 7, the influence of polynomial coefficients on tooth surface topology on both sides can be intuitively observed. However, due to various errors (such as helix angle error, pressure angle error, torsion error, tooth length curvature error and tooth profile curvature error) are mixed together. At the same time the influence of polynomial coefficients on the topological structure of the tooth surface is microscopic, the degree and weight of the influence of each order polynomial coefficient on the tooth surface cannot be effectively judged. In order to more accurately grasp the influence of each order coefficient of the motion axis polynomial on the tooth surface topology on both sides, the tooth surface deviation was expressed as equation (10) and corresponding coefficients are shown in Table 4.

$$Z = a_1X + a_2Y + a_3XY + a_4X^2 + a_5Y^2, \tag{10}$$

where a_1 is influence coefficient of helix angle error, a_2 is influence coefficient of pressure angle error, a_3 is influence coefficient of tooth surface twist, a_4 is influence coefficient of tooth length curvature, a_5 is influence coefficient of tooth profile curvature.

As Table 4 showed, the influence of the axis polynomial coefficients of the same order on the tooth surface from large to small is: pressure angle, helix angle, twist, tooth profile curvature, and tooth length curvature. For pressure angle and helix angle, the influence of the same-order coefficient on the concave surface is weaker than that on the convex surface, while for twist, tooth profile curvature and tooth length curvature, the influence of the same-order coefficient on the concave surface is stronger than the influence on the convex surface. And the trend was consistent with Figure 7.

The other influence of motion coefficients on tooth surface topology was also been analyzed. Through above analysis, the basic influence trend and rule of polynomial coefficient's change on tooth surface was clear which can be a guide to reduce tooth surface deviation.

3.3 Six-order motion expression solution

The tooth surface deviation between theoretical Σ_1 and real after ration Σ_3 can be expressed as

$$\Delta r = \boldsymbol{r}_w = \boldsymbol{r}_w(a_{ij} + \Delta a_{ij}), \tag{11}$$

where a_{ij} represent the polynomial coefficient, i represents axes of X, Y, Z, C, j(0,1,2,3,4,5,6) represents the orders of polynomial coefficient, and in above order, the coefficient is denoted as p.

The derivative and simplification of equation (11) can be obtained

$$\delta(\Delta\boldsymbol{r}).\boldsymbol{n}_w = -(\frac{\partial \boldsymbol{r}_w.\boldsymbol{n}_w}{\partial a_1} \times \partial(\Delta a_1) + \cdots + \frac{\delta \boldsymbol{r}_w\cdot\boldsymbol{n}_w}{\partial a_p} \times \delta(\Delta a_p)). \tag{12}$$

Then dot theoretical normal vector $\boldsymbol{n_w}$ in both sides of (12)

$$\delta(\Delta\boldsymbol{r}).\boldsymbol{n}_w = -(\frac{\partial \boldsymbol{r}_w.\boldsymbol{n}_w}{\partial a_1} \times \delta(\Delta a_1) + \cdots + \frac{\partial r_w\cdot n_w}{\partial a_p} \times \delta(\Delta a_p)), \tag{13}$$

where $\delta.(\Delta r)\boldsymbol{n_w}$ represents the tooth surface deviation, $(\partial \boldsymbol{r}_w\cdot\boldsymbol{n}_w)/\partial a_p$ represents sensitivity coefficient of tooth surface deviation corresponding to coefficient.

Let $\Delta\delta{=}\delta(\Delta\boldsymbol{r}).\boldsymbol{n}_w$ represents the tooth surface deviation of grid point on the tooth surface, and then the sensitivity coefficient η_p corresponding to coefficient p can expressed as

$$\eta_p = \Delta\delta/\Delta a_p. \tag{14}$$

Assuming total quantity of grid points is q, the corresponding tooth surface deviation can be represented by matrix as

$$\begin{pmatrix} \Delta\delta_1 \\ \Delta\delta_2 \\ \Delta\delta_3 \\ \cdots \\ \Delta\delta_q \end{pmatrix} = \begin{pmatrix} \eta_{11} & \eta_{21} & \eta_{31} & \cdots & \eta_{p1} \\ \eta_{12} & \eta_{22} & \eta_{32} & \cdots & \eta_{p1} \\ \eta_{13} & \eta_{23} & \eta_{33} & \cdots & \eta_{p3} \\ \cdots & \cdots & \cdots & \cdots & \cdots \\ \eta_{1q} & \eta_{2q} & \eta_{3q} & \cdots & \eta_{pq} \end{pmatrix} \begin{pmatrix} \Delta a_1 \\ \Delta a_2 \\ \Delta a_3 \\ \cdots \\ \Delta a_p \end{pmatrix}, \tag{15}$$

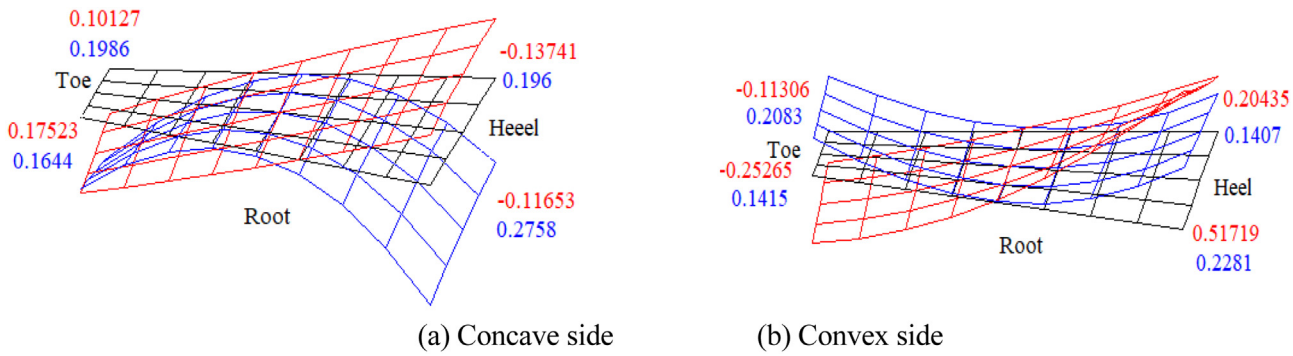

(a) Concave side (b) Convex side

Fig. 8. Tooth surface deviations of original.

where $\Delta\delta_q$ represents the tooth surface deviation of grid point q, η_{qp} is the sensitivity coefficient of the tooth surface deviation of grid point q caused by coefficient p, and Δa_p is adjustment of coefficient.

Least square method is used to solve equation (15). Therefore the adjustment of coefficients can be expressed as

$$\{\Delta a_p\} = ([\eta_{pq}]^T[\eta_{pq}])^{-1}[\eta_{pq}]^T\{\Delta\delta_q\}. \tag{16}$$

4 Examples

A numerical example is listed in Tables 1–3. Let $\psi_b = 0.438818$, then according to equations (4)–(7), the tooth suface of axis-reduced were calculated, similarly for the original tooth surface. Then based on equations (8) and (9), the tooth surface deviations between original and axis-reduced are calculated and listed in Figure 8. The blue represents the theoretical tooth surface, and the red represents the original tooth surface.

As Figure 8 shows, (a) represent deviations of concave side between theoretical and real tooth surface, (b) represent the deviations of convex side between theoretical and real tooth surface. The biggest deviations for concave side reach 0.38233 mm in the root of heel, for convex side, the biggest deviations reach 0.39415 mm in the root of toe.

Usually the elimination of tooth surface deviations is achieved by adjusting the machine tool setting parameters. While in this paper motion axes polynomial expression are adjusted to reduce the deviation. Unlike the blade can be wear to required angle by completing method, the profile angle of cutter is not repairable by five-cut method and method proposed in this paper, so the profile angle is not adjusted. Only the point radius of cutter and motion axes polynomial expression were adjusted. The point radius of cutter is 115.85 mm and 112.75 mm for inner and outer cut, adjustment polynomial expressions were listed in Table 5, and the tooth surface deviations after adjustment were showed in Figure 9.

Comparing Figures 8 and 9, after adjustment of motion axes polynomial expression coefficients, the tooth deviations were decreased. As Figure 9 shown, (a) was the tooth surface deviations after adjusted of concave side, (b) was the tooth surface deviations after adjusted of convex side. For concave side, the deviations were 0.033 mm, 0.023 mm, −0.0199 mm, and −0.0238 mm in four corners of tooth surface, the biggest deviation was 0.033 mm in the root of heel. For convex side, the deviations were 0.00507 mm, −0.0217 mm, 0.0089 mm, and 0.0309 mm in four corners of tooth surface, the biggest deviation was 0.0309 mm in the root of toe. And the closer to the midpoint of the tooth surface, the smaller the tooth surface deviations. So the theoretical tooth surfaces were approximately equivalent realized.

Based on the parameters of Table 4 and equations (4)–(7), the tooth surface points can be obtained, and 3D model by UG was shown in Figure 10.

4.1 Simulation processing

During the process, the machine procedures of two sides are optimization and adjustment as showed in Figure 11.

As Figure 11 shows, during manufacture the convex side of pinion, the inner cut and workpiece were in work (green color). The cutter moves from toe to heel of pinion with self-rotation, and the workpiece rotates clockwise around the axis. After convex side was finished, the program was switched to manufacture the convex side of pinion. In contrast, the outer cut and workpiece were in work (red color), cutter moves from heel to toe of pinion with self-rotation, and the workpiece rotates anticlockwise around the axis. As a tooth was manufactured, the workpiece index until the pinion was processed. The pinion is machined in one machine tool which eliminated multiple installations.

A simulation processing is carried out in VERICUT to improve the efficiency and to find potential errors. Based on Figure 1, a virtual prototype was established which is Five-axis four linkage spiral bevel gear machining tools. According to Table 5, the NC code was calculated and showed in left of Figure 12. The simulation was showed in the middle of Figure 12. The right of Figure 12 was enlarge image of process.

After pinion simulated, the pinion is compare to Figure 10 and the error is showed in Figure 13.

The results of Figure 10 and simulated pinion were shown in Figure 13. For convex side, the biggest tooth surface error was 0.01 mm of residue located in the toe of tooth surface. For concave side, the biggest error was

Table 5. Adjustment motion axes polynomial expression of pinion.

Items	Concave side	Convex side
C_x	$41.62239 - 180.752059.\varphi_c - 83.2447767.\varphi_c^2 + 120.501373.\varphi_c^3$ $+27.7482589.\varphi_c^4 - 24.100274.\varphi_c^5 - 3.6997678.\varphi_c^6$	$44.215944 - 192.015.\varphi_c - 88.43189.\varphi_c^2$ $+128.0100.\varphi_c^3 + 29.477296.\varphi_c^4 - 25.602.\varphi_c^5$ $-3.930306.\varphi_c^6$
C_y	$-94.25603 - 83.244777.\varphi_c + 180.75206.\varphi_c^2 + 55.496518.\varphi_c^3$ $-60.25069.\varphi_c^4 - 11.099304.\varphi_c^5 + 8.033424.\varphi_c^6$	$-93.5075 - 88.431889.\varphi_c + 192.015.\varphi_c^2$ $+58.954592.\varphi_c^3 - 64.005.\varphi_c^4 - 11.790918.\varphi_c^5$ $+8.534.\varphi_c^6$
C_z	$-97 + 0.8.\varphi_c - 0.0023.\varphi_c^2 + 0.0014.\varphi_c^3 + 0.0025375.\varphi_c^4$ $-0.0008.\varphi_c^5 - 0.00062.\varphi_c^6$	$-1.080 + 2.35.\varphi_c - 0.0017.\varphi_c^2 + 0.00036.\varphi_c^3$ $+0.00026.\varphi_c^4 - 0.0018.\varphi_c^5 - 0.00078.\varphi_c^6$
C_c	$-0.0226356 - 2.14.\varphi_c + 0.02056.\varphi_c^2 + 0.00407.\varphi_c^3$ $-0.00036.\varphi_c^4 - 0.000132.\varphi_c^5 + 0.000017.\varphi_c^6$	$-0.0226356 - 2.2150.\varphi_c + 0.01332.\varphi_c^2$ $+0.00156.\varphi_c^3 - 0.00187.\varphi_c^4 - 0.000064.\varphi_c^5$ $+0.000039.\varphi_c^6$

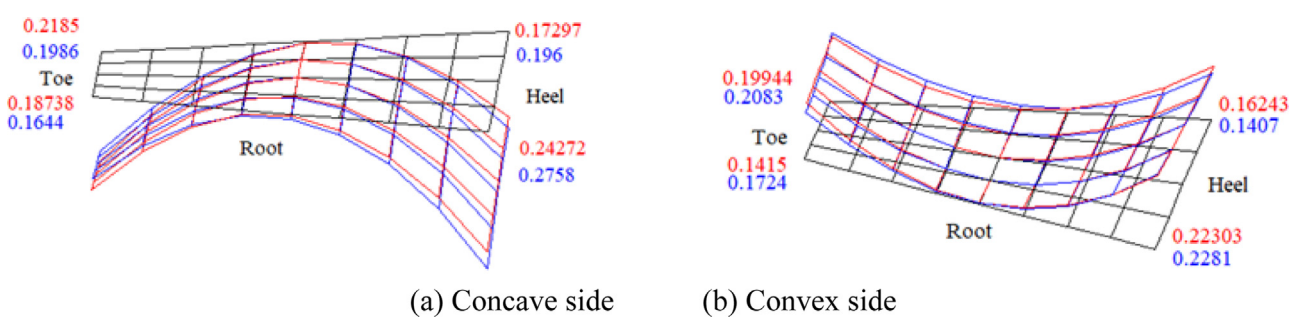

(a) Concave side (b) Convex side

Fig. 9. Tooth surface deviations after adjusted.

0.01 mm of overcut located in the middle of tooth surface. The error may be caused by modeling accuracy or decimal points in the calculation process. However, the precision of tooth surface displayed meet engineering requirements.

The planning of machining path is verified by simulating machining, which can effectively avoid the possible interference. The NC code can be used to cut experiment.

4.2 Cut experiment

A five-axis four linkage CNC milling machine as shown in Figure 14 were used to machine by simulated NC code. The cutting process was stable without vibration, and the scene of tooth cutting was shown in Figure 15.

Due to the influence of various errors (such as machine tool error, workpiece installation error and cutter, etc.), there is a certain error between the processed tooth surface and the theoretical tooth surface. It is inevitable to measure tooth surface to ensure the quality of tooth surface. The result was shown in Figure 16.

As shown in Figure 16, for concave side, the biggest error is 10.4 μm at the root of toe, and for convex side, the biggest error is 14.8 μm at the top of toe. While the errors almost no impact on the contact performance of the tooth surface and the accuracy meets engineering requirements.

Finally a rolling test was carried out. The pair ran smoothly without obvious noise and the results of contact patterns were in Figure 17.

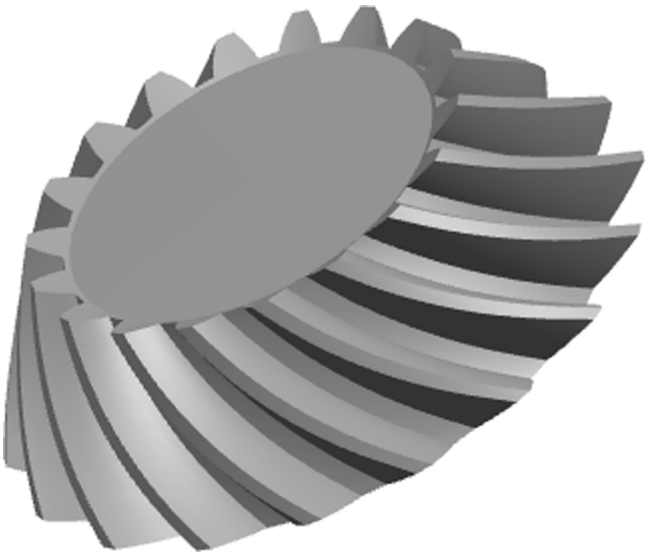

Fig. 10. 3D model of pinion.

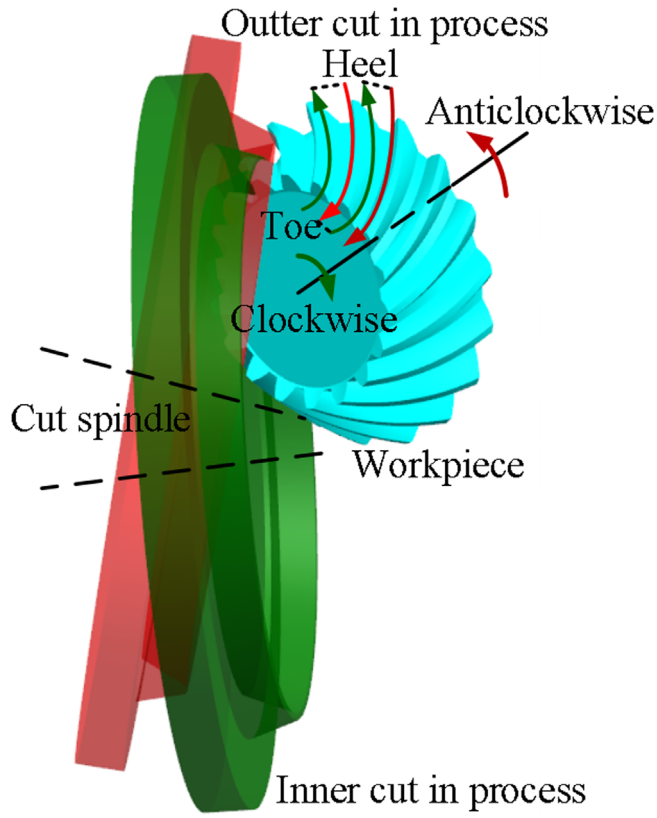

Fig. 11. Cutting process by equivalent completing method.

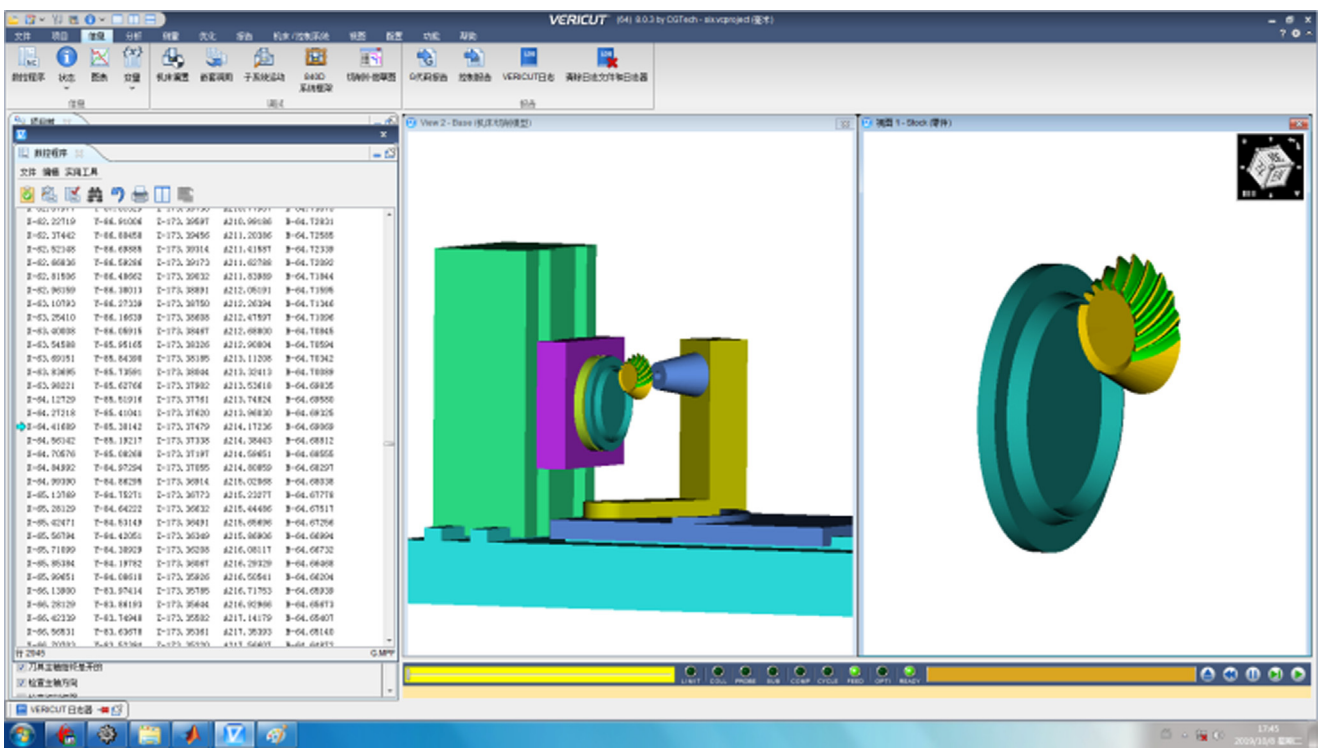

Fig. 12. Simulation processing.

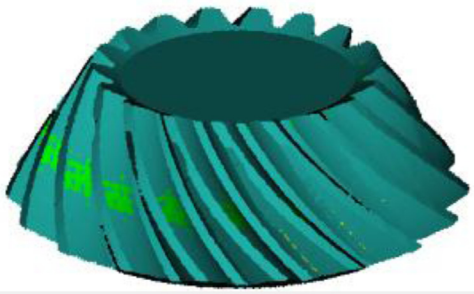

Overcut		Residue	
Range	Color	Range	Color
0.10000	49:Firebrick	0.10000	62:Machine_2
0.05000	11:Violet Red	0.05000	61:Machine_1
0.04000	55:AutoDiff_G5	0.04000	60:AutoDiff_E5
0.03000	54:AutoDiff_G4	0.03000	59:AutoDiff_E4
0.02000	53:AutoDiff_G3	0.02000	58:AutoDiff_E3
0.01000	52:AutoDiff_G2	0.01000	56:AutoDiff_E1
0.00500	51:AutoDiff_G1	0.00500	57:AutoDiff_E2
0.00000	7:Light Sea Green	0.00000	7:Light Sea Green

Fig. 13. Results of compare.

Fig. 14. Machine prototype.

As Figure 17 display, (a) is the scene of rolling test, (b) is the real contact pattern for gear convex, (c) is the real contact pattern for gear concave. For convex side the contact path is from the topland of heel to the root of toe, and for concave side the contact path is from the root of heel to the topland of toe. For both concave and convex side of gear the contact pattern are located in the middle of tooth surface. Tooth surface contact patterns meet engineering requirements. Application example shows the effectiveness and feasibility of the method.

Fig. 15. Cut experiment.

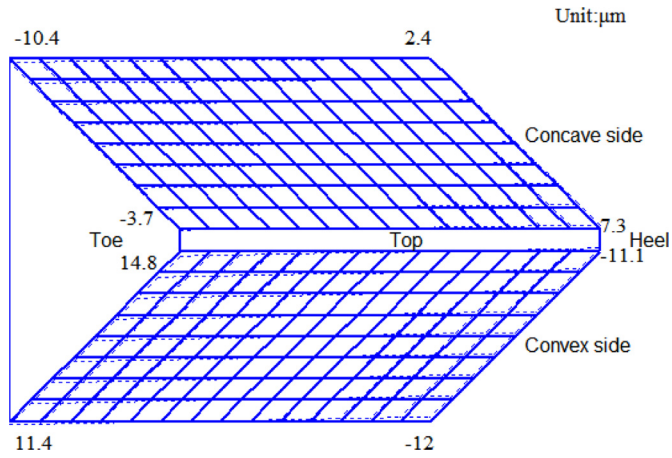

Fig. 16. Measure result.

5 Conclusion

In this paper the advantages and disadvantages of five-cut method and completing method are analyzed firstly, then an equivalent completing method by four-axis dedicated spiral bevel gear milling machine is proposed which overcomes shortcomings of the five-cut method and completing method.

The machine setting parameters are equivalent to the motion axis polynomial of five-axis CNC milling machine, and spiral bevel gear can be machined without machine root angle change during process by adjusting the polynomial coefficient. Through the reasonable planning of the machining process, spiral bevel gear is machined in one clamp by dedicated spiral bevel gear milling machine. The research results of this paper enrich the method to machine spiral bevel gears.

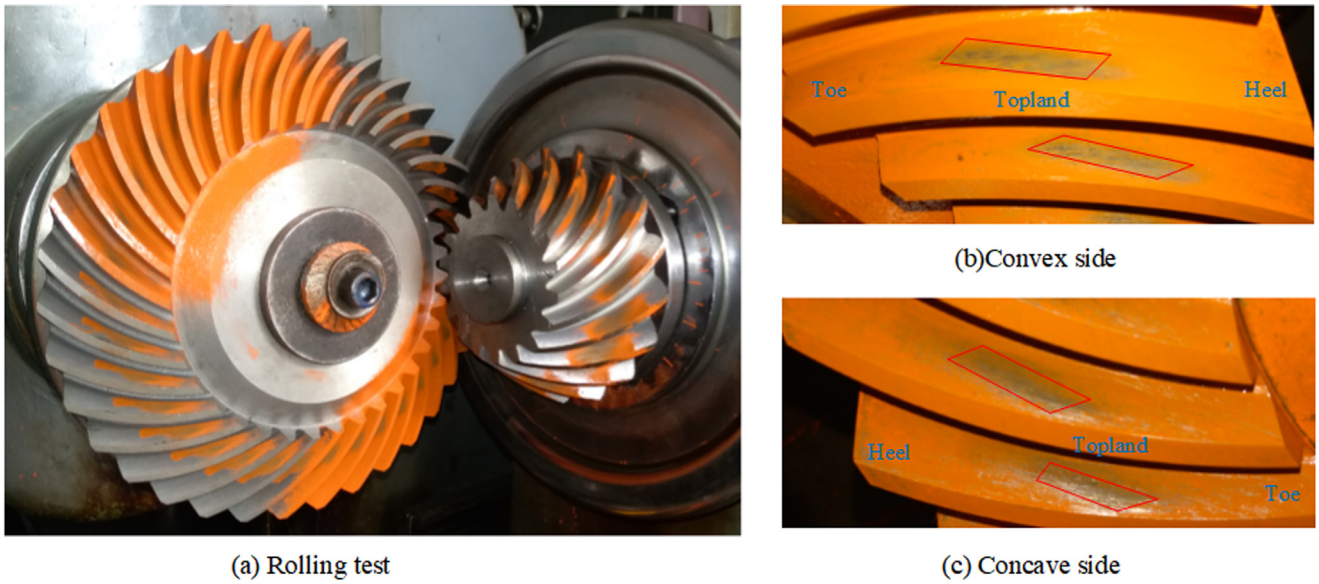

Fig. 17. Result of rolling test.

Funding

The research is funded by Henan Provincial Science and Technology Research Project (Grant No. 242102220084) and the National Natural Science Foundation of China (Grant Nos. 51475141, 51705134).

Conflicts of interest

The authors declare that they have no competing interests.

Data availability statement

All data generated and analyzed during this study are included in this article.

Author contribution statement

Longlong Geng, Shaowu Nie, Chuang Jiang proposed the method and established model, Longlong Geng, Chuang Jiang contributed to the calculation, analysis, and cut experiment, Longlong Geng, Shaowu Nie and Chuang Jiang contributed to writing—original draft preparation, all the authors contributed to writing, review, and editing, Longlong Geng and Shaowu Nie acquired the funding.

References

[1] F.L. Litvin, A. Fuentes, K. Hayasaka. Design, manufacture, stress analysis, and experimental tests of low-noise high endurance spiral bevel gears, Mech. Mach. Theory **41**, 83–118 (2006)

[2] H.J. Stadtfeld, Tribology aspects in angular transmission systems: hypoid gears, Gear Technol. 66–72 (2011)

[3] B.A. Shtipelman, Design and Manufacture of Hypoid Gears, A Wiley-Interscience Publication, New York (1978)

[4] F.L. Litvin, Y. Zhang, Local synthesis and tooth contact analysis of face-milled spiral bevel gears, Tech Rep. National Aeronautics and Space Administration, Cleveland (1991)

[5] F.L. Litvin, A.G. Wang, Local synthesis and tooth contact analysis of face-milled, uniform tooth height spiral bevel gears, Tech Rep. National Aeronautics and Space Administration, Cleveland (1996)

[6] Z.C. Chen, M. Wasif, A generic and theoretical approach to programming and post-processing for hypoid gear machining on multi-axis CNC face-milling machines, Int. J. Adv. Manuf. Technol. **81**, 135–148 (2015)

[7] Gleason Works Calculation Instructions Generated Hypoid Gears Duplex Helical Method, the Gleason Works, New York (1971)

[8] F.L. Litvin, Y. Gutman, Methods of synthesis and analysis for hypoid gear-drives of "formate" and "helixform"—Calculations for machine settings for member gear manufacture of the formate and helixform hypoid gears, J. Mech. Des. **103**, 83–110 (1981)

[9] Y. Zhang, H.Z. Yan, New methodology for determining basic machine settings of spiral bevel and hypoid gears manufactured by duplex helical method, Mech. Mach. Theory **100**, 283–295 (2016)

[10] L.L. Geng, X.Z. Deng, J. Deng et al., Calculation and experiment of spiral bevel gear by duplex helical method predesigned contact path, J. Adv. Mech. Des. Syst. Manufactur. **15**, 1–17 (2021)

[11] X.Z. Deng, G.G. Li, B.Y. Wei, J Deng, Face-milling spiral bevel gear tooth surfaces by application of 5-axis CNC machine tool, Int. J. Adv. Manuf. Technol. **71**, 1049–1057 (2014)

[12] L.L. Geng, X.Z. Deng, X.M. Cao et al., Research on calculation of machine-tool settings and flank modification for spiral bevel gear by duplex spread blade method based on 4-axis CNC milling machine, J. Adv. Mech. Des. Syst. Manufactur. **14**, 1–16 (2020)

[13] L.L. Geng, X.Z. Deng, H. Zhang et al., Theory and experimental research on spiral bevel gear by double-side milling method, Mech. Ind. **22**, 1–11 (2021)

[14] J. Deng, C. Jiang, X.Z. Deng et al., The optimal calculation and machining of the spiral bevel gear pinion based on the same cutter head, J. Adv. Mech. Des. Syst. Manufactur. **14**, 1–16 (2020)

[15] H.J. Stadtfeld, U. Gaiser, The ultimate motion graph, J. Mech. Des. **122**, 317–322 (2000)

[16] P.Y. Wang, Z.H. Fong, Fourth-order kinematic synthesis for face-milling spiral bevel gears with modified radial motion (MRM) correction, J. Mech. Des. **128**, 457–467 (2006)

[17] Q. Fan, Tooth surface error correction for face-hobbed hypoid gears, J. Mech. Des. **132**, 011004 (2010)

[18] Y.P. Shih, Z.H. Fong, Flank correction for spiral bevel and hypoid gears on a six-axis CNC hypoid generator, J. Mech. Des. **130**, 062604 (2008)

[19] Y. Yang, S.M. Mao, A method to process spiral bevel gear by completing (2018) CN109101754A

[20] Y. Yang, S. Mao, B. Bai, Y. Kuang, Active design and manufacture of face-milled spiral bevel gear by completing process method with fixed workpiece axis based on a free-form machine tool, Int. J. Adv. Manufactur. Technol. **112**, 2925–2942 (2021)

[21] S.W. Nie, C.F. Lai, S.C. Tang et al., Tooth flank modification method for pinion of spiral bevel gears without tilt processing, J. Henan Univ. Sci. Technol. **41**, 12–17 (2020)

[22] Y.P. Shih, Z.H. Sun, K.L. Lai, A flank correction face-milling method for bevel gears using a five-axis CNC machine, Int. J. Adv. Manuf. Technol. **91**, 3635–3652 (2017)

Cite this article as: L. Geng, S. Nie, C. Jiang, A method to manufacture spiral bevel gears by equivalent completing, Mechanics & Industry **25**, 18 (2024)